Evaluation of Ethane as a Power Conversion System Working Fluid for Fast Reactors

by

Jeffrey A. Perez

Submitted to the Department of Nuclear Science and Engineering in Partial Fulfillment of the Requirements for the Degree of

Bachelor of Science in Nuclear Science and Engineering
at the
Massachusetts Institute of Technology

June 2008

Signature of Author: ....
Jeffrey A. Perez
Department of Nuclear Science and Engineering
May 8, 2008

Certified by: ....
Dr. Michael Driscoll
Professor Emeritus of Nuclear Science and Engineering
Thesis Supervisor

Certified by: ....
Dr. Pavel Hejzlar
Principal Research Scientist
Thesis Reader

Accepted by: ....
Dr. David Cory
Professor of Nuclear Science and Engineering
Chairman, NSE Committee for Undergraduate Students

Evaluation of Ethane as a Power Conversion System Working Fluid for Fast Reactors

by

Jeffrey A. Perez

Submitted to the Department of Nuclear Science and Engineering on May 9, 2008
in partial fulfillment of the requirements for the Degree of
Bachelor of Science in Nuclear Science and Engineering.

ABSTRACT

A supercritical ethane working fluid Brayton power conversion system is evaluated as an alternative to carbon dioxide. The HSC® chemical kinetics code was used to study thermal dissociation and chemical interactions for ethane and other coolants under a variety of conditions. The NIST database was used for reaction rates. Overall results were not conclusive. The supercritical behavior of ethane at high pressures is not well documented, and the recombination rates of its dissociation reactions could prove very important. Ethane is known to crack into ethylene, but computer simulations show that it can, at equilibrium, also form significant amounts of hydrogen and methane. These reactions cracked more than 25% of the ethane above 300°C, even though high (20 MPa) pressure significantly reduced dissociation compared to results at 0.1 MPa. At high pressure it appears that ethane might recombine much faster than it dissociates, which would be highly advantageous. Further research and experimentation is encouraged. Simple experiments should be sufficient to identify the behavior of ethane at high temperatures and pressures.

Ethane was calculated to have better heat transfer properties than carbon dioxide. In particular, heat exchanger sizes could be reduced by as much as a factor of three. On the other hand, more turbomachinery stages are needed.

A simple experiment is proposed to determine whether recombination under compressor inlet conditions is sufficiently fast and complete to make the use of ethane a practical proposition.

The chemical reaction of ethane with sodium, while it generates hydrogen, is endothermic, which may quench the reaction in the event of small heat exchanger leakage.

Thesis Supervisor: Professor Michael Driscoll
Title: Professor Emeritus of Nuclear Science and Engineering

Acknowledgements

I would first and foremost like to thank my parents without whose love and support I would not be where I am today. I want them both to know how much I love them and appreciate all that they have done and sacrificed for me.

I would also like to sincerely thank Professor Michael Driscoll for all of the help that he has given me in this process. In every step along the way, his insights and feedback have been crucial to my success. He has been patient, understanding and supportive, and for that I am incredibly grateful. I would also like to thank Dr. Pavel Hejzlar who has also provided feedback and suggestions throughout the thesis writing process.

Table of Contents

List of Figures

List of Tables

1. Introduction

1.1 Background and Motivation

The liquid metal cooled fast breeder reactor (LMFBR) features prominently in future nuclear power growth scenarios. It is the central focus of the US-led Global Nuclear Energy Partnership (GNEP) [1] and of a recently awarded NERI project at MIT [2]. A power conversion system (PCS) consisting of a steam cycle, as is used in most current reactors, is unappealing for LMFBRs because they are typically cooled by liquid sodium, and any leak between the two systems could have catastrophic consequences. So a less reactive secondary coolant is desired.

Currently supercritical CO_2 is the predominant choice of working fluid for use in closed Brayton cycle power conversion systems. Extensive research has been done on the CO_2 cycle [1], and it provides significant advantages over helium, its main competitor. Namely, it offers comparable performance at lower temperatures. Other materials might have the potential, however, to offer even better material or thermodynamic properties.

Since balance of plant can constitute a significant portion of the cost of a plant, increases in efficiency can mean smaller components and an overall reduction in cost.

1.2 Objectives of Present Work

Ethane (C_2H_6) is evaluated as a potential replacement for CO_2 as a PCS working fluid for use with a LMFBR. In order for ethane to be considered, it must offer performance comparable to that of carbon dioxide. CO_2 is less reactive with sodium than water, and it is able to operate at high power cycle efficiency and much lower temperatures than helium [1], meaning that it is applicable in a wider variety of situations. Ethane, therefore, should be comparable in these regards.

Ethane is considered for several reasons: its critical temperature is very close to that of CO_2 and there has been extensive research done on it. In order to be a viable competitor, another material must have a critical temperature near that of CO_2. If that is the case, then the law of corresponding states, which roughly correlates properties according to critical temperatures and pressures, suggests that, at least to first order, the two materials are highly substitutable. A critical temperature near ambient is desirable because the work consumed by Brayton cycle compressors is significantly reduced compared to ideal gas working fluids [1]. A summary of critical properties of carbon dioxide and ethane is shown in Table 1.1. Ethane is well researched because it has several industrial uses. At low temperatures it is used as a refrigerant, and at high temperatures it is cracked to produce ethylene. So there should be sufficient data already available to make a preliminary analysis possible.

Table 1.1 – Comparison of Material Properties

	CO_2	C_2H_6	Ratio C_2H_6/ CO_2
Molecular Weight	44.01	30.07	0.683
Critical Pressure (MPa)	7.377	4.89	0.663
Critical Temp. (C)	31	32.2	1.04
Critical Density (kg/m^3)	467.6	203	0.434

Its two most serious drawbacks are its flammability and potential for thermal decomposition. Ethane is one of the principle constituents of natural gas, and therefore is highly flammable. Savings from efficiency would therefore have to be sufficient to outweigh the potential costs of working with a more hazardous material.

If for no other reason, an investigation of ethane should be instructive in that it will elucidate the reasons for carbon dioxide's predominance as the choice of coolant.

1.3 Description of HSC Code

HSC Chemistry® 6.0 is a code designed for chemical reaction and equilibria calculations. It has several independent modules, and the one primarily used in this report is the Equilibrium Module. This tells the end products of a reaction, given the initial reactants, at equilibrium. It takes input in the form of all chemical compounds to be considered in a reaction (reactant and product) and operating parameters such as ambient pressure and temperature. The program makes clear that careful definition of the chemical reaction and potential products is crucial: "The most demanding step is the selection of the species and phases, ie. the definition of the chemical system."[3]

It then uses a Gibbs energy minimizing algorithm to find the most stable combination of all the given compounds and elements. It gives the amount of each selected compound at equilibrium as well as the change in free energy and entropy associated with the reaction. All data in this report examines a fixed amount of reactants at varying pressures and temperatures, though it is possible to simulate addition of material at fixed conditions. A sample of an HSC output is shown in Appendix B.

HSC does not take into account rate effects or non-ideal conditions, and for this reason its results should be understood to be idealized representations of solutions.

1.4 Organization of This Report

Chapter 2 first examines the thermal dissociation of ethane. Since high temperature and pressure performance are necessary, this is of paramount importance. HSC is used to evaluate ethane in a variety of temperature and pressure conditions, and various dissociation schemes are analyzed. Then reaction rate effects are considered, and finally, material damage by radiation in the form of radiolysis is studied.

Chapter 3 looks at how reactive ethane is relative to other secondary coolants. First the reactions between sodium and various secondary coolants are compared. Then reactions are evaluated between ethane and sodium and liquid salts, both of which are also currently under consideration as primary coolants.

Chapter 4 gives a preliminary examination of scaling for various components including heat exchanger and turbomachinery.

Chapter 5 provides a summary of important results and conclusions, and recommends future work.

Data for all figures and calculations throughout can be found in Appendix A.

2. Ethane Stability

2.1 Chapter Introduction

Using ethane as a PCS secondary coolant requires that it maintain chemical stability at the pressures and temperatures of operation. In order for it to be a viable competitor with the other options already available, it must be shown that it does not break down, as doing so would significantly alter its useful chemical properties. This chapter will look at the thermal dissociation of ethane at several levels of complexity, the time rates associated with these reactions, and finally at radiolysis, another potential loss mechanism for coolant.

2.2 Ethylene Production

One of the most common current uses for ethane is in the production of ethylene. Worldwide, ethane is the second most common material used to produce ethylene, and its use is increasing. The process of converting heavier hydrocarbons to ethylene is known as hydrolysis or steam cracking. In this process the ethane, along with water to lower partial pressure, is heated to 500-650°C, and then repeatedly and briefly increased to temperatures as high as 850°C, where bonds are broken and smaller molecules formed. "Ethylene is the largest-volume petrochemical produced worldwide [4]," and as such there has been much research done on its production and, more specifically, the ethane reaction used to produce it [4].

The formation of ethylene depends on three factors: high temperature, low pressure, and short residence time. High temperatures are needed to promote the endothermic reactions that govern cracking. Low pressure and residence times are necessary because of the nature of ethylene. If it is allowed to stay at high pressures or high temperatures for too long, it will tend to react to produce other, secondary, products, which are not desired.

2.3 PCS Cracking

The present object of investigation, however, is the use of ethane as a supercritical power conversion system (PCS) working fluid. In this case cracking is not desirable; it would effectively reduce the amount of working fluid in the system and change its properties, particularly near the critical point. The PCS system operates at moderately high temperatures (550-650°C) but, unlike the cracking reactor, at high pressures. The high temperature acts to promote cracking, but the high pressure acts to suppress it. It is not immediately obvious which of these effects is dominant, so it is important to verify whether, at the intended operating conditions, there is a significant amount of dissociation.

The chemical thermodynamics code, HSC [3], was used to do this evaluation. The HSC code analyzes a set of given chemical compounds at given temperature and pressures and uses a Gibbs energy minimization method to identify the most stable combination [3]. Preliminary analysis verified that at conditions found in ethane cracking reactors full dissociation of ethane occurs. The supporting data for this reaction is found in appendix A.2.0.

Since ethane (C_2H_6) is known to dissociate into ethylene (C_2H_4), HSC was first used to check for dissociation according to equation (1).

$$C_2H_6 \leftrightarrow C_2H_4 + H_2 \qquad (2.1)$$

These calculations were done in two ways: at a constant pressure of 20 MPa, varying temperature from 423-923°K (Figure 2.1), and at a constant temperature of 823°K, varying pressure from 0.1 to 20 MPa (Figure 2.2).

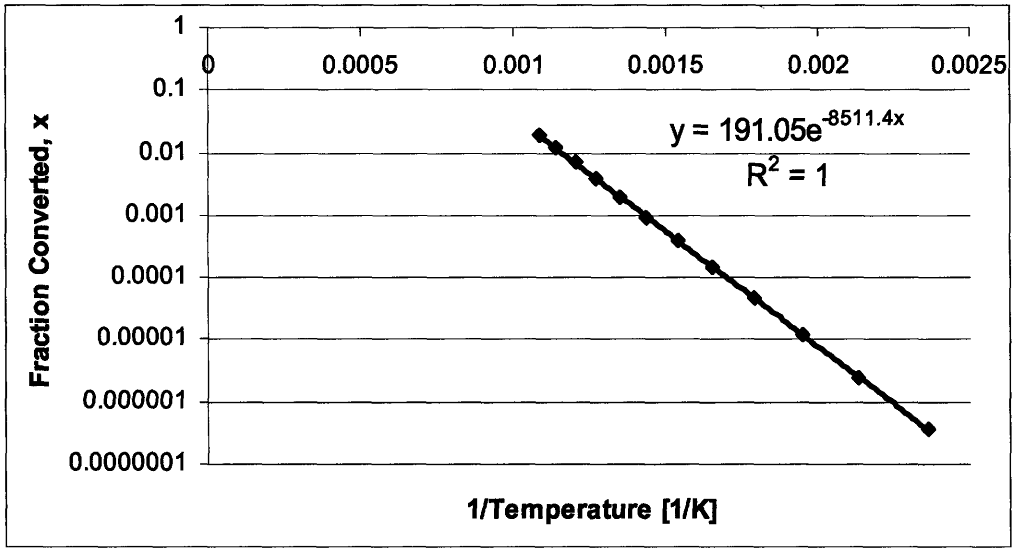

Figure 2.1: Fraction of Ethane Cracking vs. 1/Temperature at 20 MPa

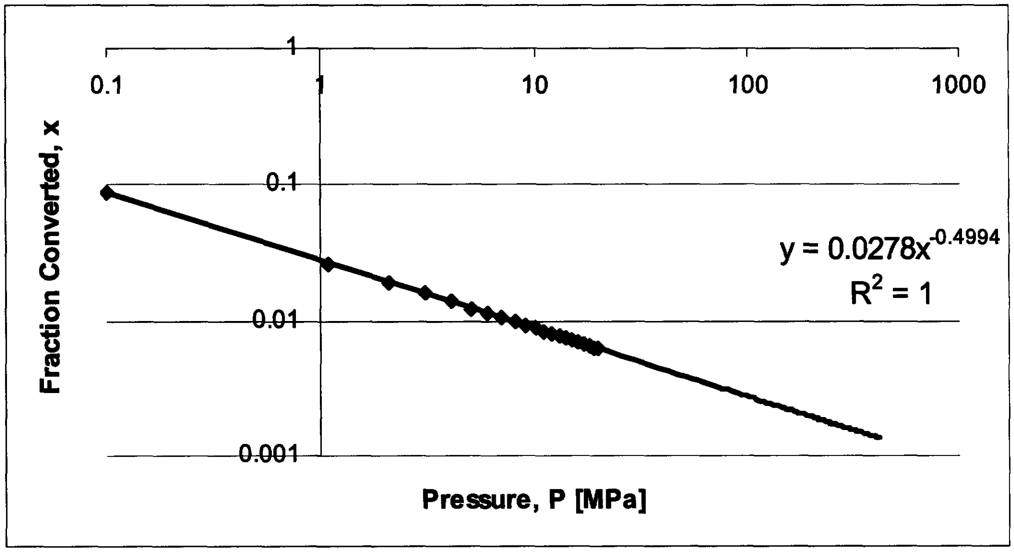

Figure 2.2: Fraction of Ethane Cracking vs. Pressure at 550°C

These plots show that the amount of ethane cracking at the point of interest (550°C and 20 MPa) is ~0.6%. This is well below a tolerable value for power cycle applications. Curve fits to this data give the dissociation fraction, x, as functions of T and P:

$$x=191*e^{-8511/T} \tag{2.2}$$

$$x=0.0876/P^{0.5} \tag{2.3}$$

These functions fit what is theoretically expected for a dissociation reaction, and therefore, also serve as another check on the validity of the program. In Reference [5], figure 2.3 shows that empirically, these are the relationships that ought to hold.

2.4 Extra Decay Modes

While at the conditions at which commercial ethylene production takes place, equation (2.1) is dominant, it is worth demonstrating that other possible byproducts are not produced. Ethane cracking is a known and reliable method for creating ethylene, but it does not necessarily follow that at the significantly different pressures and time scales under review different chemical reactions might become more prevalent.

Equation (2.1) is a simplified representation of the ethane to ethylene reaction, and this simplification creates uncertainty about potential byproducts. The free radical mechanism predicts production of CH_4, C_2H_6, C_3H_8, C_4H_{10}, and others in the cracking of ethane [4]. This method describes the entire chain of reactions involved in the production of ethylene. Equation (2.1) is replaced by the series of reactions described in equations 2.4 – 2.11 [11]. It is unclear, however, if these three equations represent the only pathway, or merely one of several. It is noted that "the mechanisms proposed generally include the following reactions." This, at least, gives the appearance that the full mechanism is not understood or agreed upon, but these reactions are fairly standard.

$$C_2H_6 \rightarrow CH_3^* + CH_3^* \quad (2.4)$$

$$CH_3^* + C_2H_6 \rightarrow CH_4 + C_2H_5^* \quad (2.5)$$

$$C_2H_5^* \rightarrow C_2H_4 + H^* \quad (2.6)$$

$$H + C_2H_6 \rightarrow C_2H_5 + H_2 \quad (2.7)$$

$$C_2H_5 + C_2H_5 \rightarrow C_4H_{10} \quad (2.8)$$

$$C_2H_5 + C_2H_5 \rightarrow C_2H_4 + C_2H6 \quad (2.9)$$

$$H + C_2H_5 \rightarrow C_2H_6 \quad (2.10)$$

$$C_2H_5 + CH_3 \rightarrow C_3H_8 \quad (2.11)$$

Section 3 of the same report [11] makes it explicitly clear that Equations 2.6 and 2.7 have associated reverse reactions, but does not elaborate about others.

In a run that checks for all but the heavier hydrocarbon chains, there are some surprising results. Figure 2.3 shows the amount of each compound considered that results from thermal dissociation of ethane at various temperatures; all results are at 20 MPa. The ethane experiences significant degradation, though not into ethylene as was expected. It breaks down predominantly into methane, but it also produces ethylene to a greater extent than when considering equation (1) alone. This result follows from equations 2-4, which shows that every molecule of ethylene produced should also produce one of methane. The Ullman reference does not, however, clarify whether this free radical representation is the only one, or if there are alternate paths to ethylene production. Other free radical pathways might explain why it is possible to commercially crack ethane without producing methane.

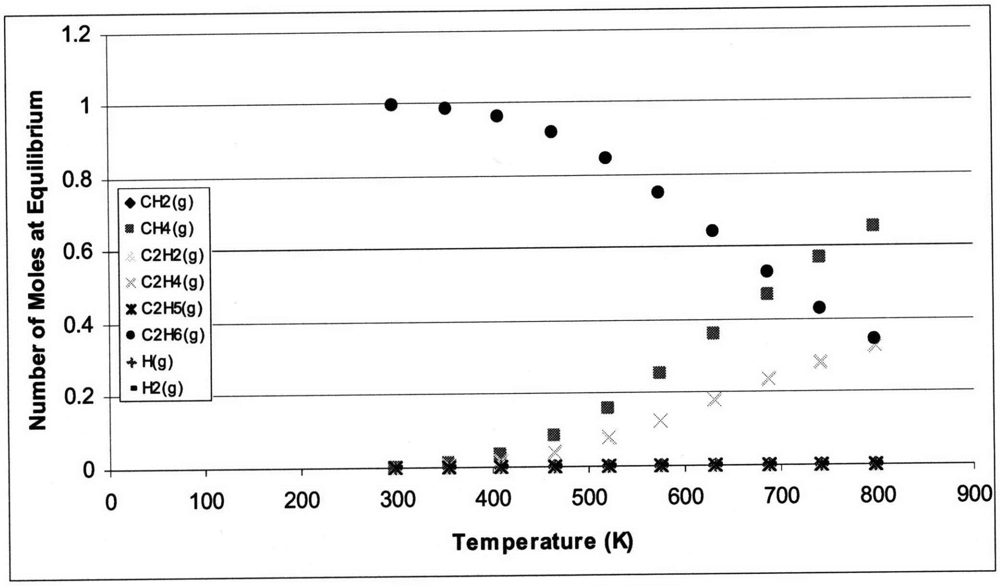

Figure 2.3: Decomposition of 1 mol of Ethane

This is seriously detrimental to the prospects of an ethane PCS. The critical temperature of methane is -82°C, compared with 32°C for ethane [6]. As was mentioned in the introduction, critical temperatures must be close in order for the law of corresponding states to apply. If some small portion of the ethane had cracked it would not have been sufficient to significantly alter the material properties, but if more than half of it is breaking down (which is the case at ~700°K) then it appears that the ethane would not be a workable option. These results, however, stand in opposition to other research and industrial practices. It is possible that there is some other process or effects at work.

2.5 Rate Effects

The reason for the disparity between these calculations and the known reality of cracking ethane to produce ethylene is likely the relative reaction rates. Ethane cracking plants usually only heat up the gas to the peak temperatures for very short times (on the order of seconds). Since the HSC code that was used only looks at free energy minimization, and all results are given at equilibrium, it is likely that the ethane to ethylene reaction occurs much quicker than the ethane to methane one. In this way, it is possible to produce ethylene without simultaneously producing methane if it is done quickly, before the mixture is allowed to come to equilibrium. If this is the case, then an ethane PCS would require more research and likely experimentation.

The actual situation may not be as serious as Figure 2.3 might suggest. Depending on how rapidly equilibrium is achieved, it may well be that dissociation is not a serious limitation. The key condition for cycle performance is at the compressor inlet, which is about 35°C (308 K), where dissociation is negligible. However if cycle average temperature dominates dissociation could be too severe. To settle this issue dynamic molecular simulation and loop tests will be required.

The NIST database provides limited reaction data for the various cracking modes of ethane. Figures 2.4 and 2.5 show NIST data for the ethane to CH_3 reaction (equation 2.4), which was available over the widest range of temperatures. Figure

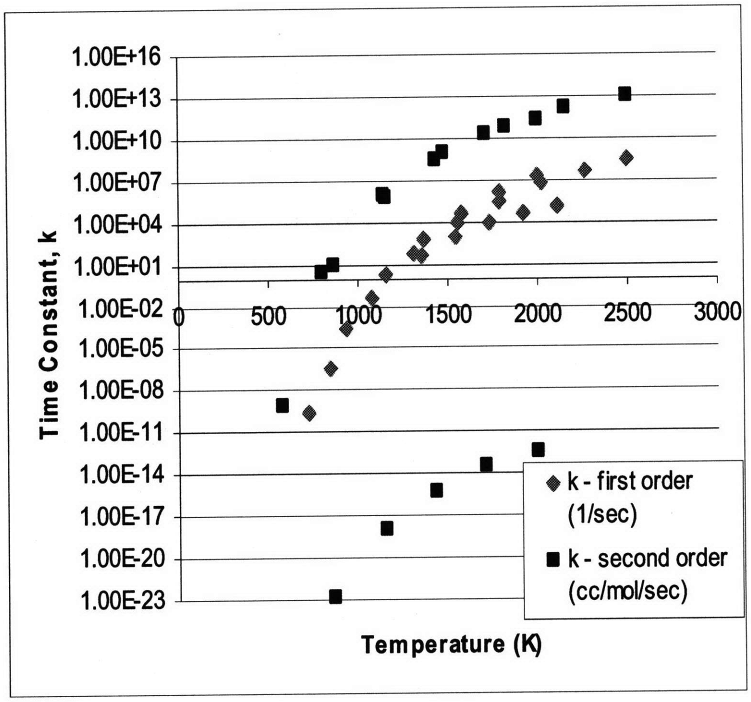

Figure 2.4: Time Constants for Ethane Cracking into CH_3

2.4 shows first and second order time constants for the reaction. The first order constants have units of sec^{-1} and correspond to the forward reaction; the second order ones have units of cm^3/mol/sec and correspond to the reverse reaction. Of particular interest in this figure are the second order values appearing both above and below the first order. This belies a profound lack of understanding for the process. Both of these data sets come from the NIST database (more information is found in appendix A.2.4), and both are based on literature review. Unfortunately second order experimental data are rare and often cover only a small specific temperature range.

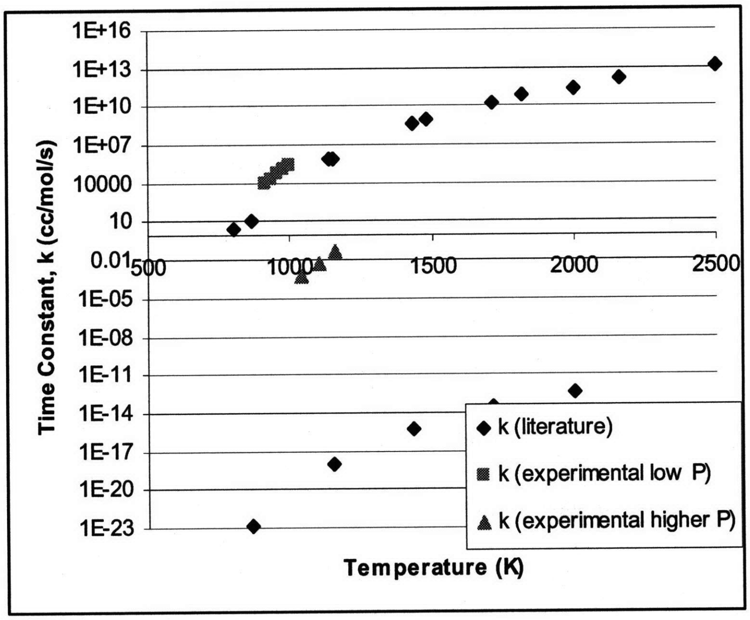

Figure 2.5: Experimental and Theoretical Time Constants For the Recombination of Ethane

Figure 2.5 shows the same two literature-based second order data sets as figure 2.4. In addition it also contains the two sets of experimental data given by NIST. These two were obtained by gas chromatography, and are interesting for several reasons. The upper experimental data is from experiments performed between 1.34E-4 and 2.66E-2 MPa, and the lower at 0.1 MPa. This confirms, as was suspected, that increasing pressure pushes the reaction in the reverse direction as well as increasing the rate at which it goes. Also, the experimental data was taken in a static or low flow situation, which is not the condition which would be under investigation ideally. It should be kept in mind that all this data applies to equation 2.4, which is the first step in the chain of reactions to create ethylene. These are important because they give an indication of the rate of the overall process. However, they do not necessarily describe equation 2.1, the production of ethylene, which is of principal interest. NIST offers only three data sets on this reaction and they all apply only to small temperature ranges. These are shown in Figure 2.6.

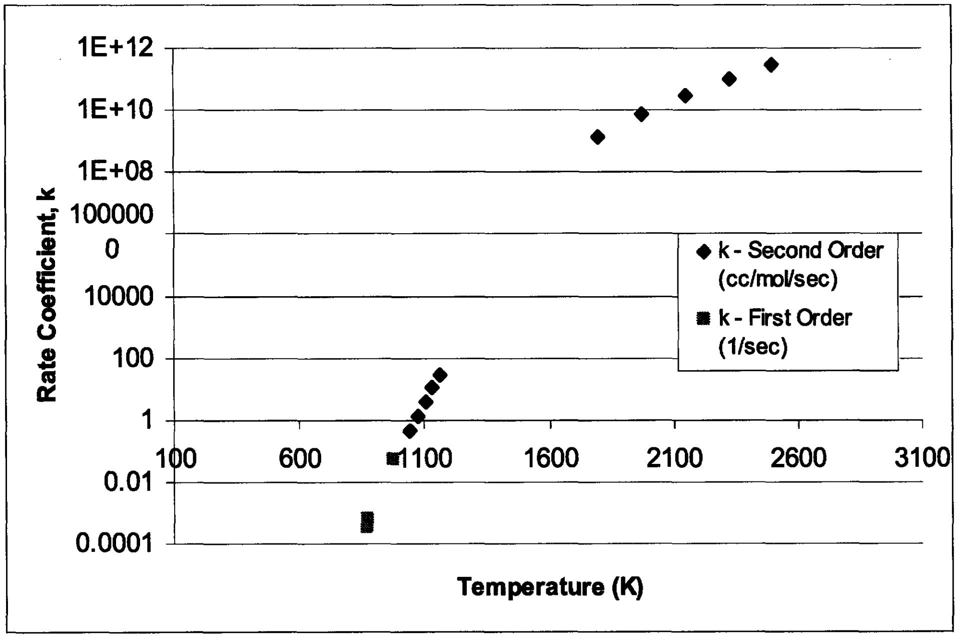

Figure 2.6: Experimentally-Derived Rate Constants for Ethylene Production

Again these data were collected at pressures around 1 atm, and first order data are insufficient to give any idea of a larger trend. Taken in conjunction, the last three figures, indicate that there is a possibility that, even if ethane cracks at high pressure and temperature regimes, it will recombine more quickly. In all, more research and experimentation will be needed to find out definitively how ethane will behave.

2.6 Carbon Dioxide Dissociation

HSC runs were done on CO_2 for temperatures below 973 K at a constant pressure of 200 bar. These indicate that carbon dioxide does not undergo the extent of thermal degradation that ethane does. Nowhere in the tested temperature range (373-973°K) did carbon dioxide thermally dissociate to a substantial degree. At the highest degree of dissociation, the two most abundant compounds were CO which appeared at a fraction of 1E-7, and O_2 at 5E-8. Carbon dioxide appears to be thermally stable in the entire range. This appears to be one significant advantage that the CO_2 cycle has over ethane. See Appendix A.2.7

2.7. Radiolysis of Ethane

A certain amount of PCS working fluid will be degraded by radiation in the IHX during operation of the reactor, and it is important to ensure that a significant portion of the coolant is not degraded in this way. The IHX is exposed to radiation mainly from two sources: leakage from the core and activated sodium. With respect to the core periphery, gamma radiation is far more likely to affect the IHX than neutrons, so only gamma heating will be examined. For sodium, the only isotope contributing significant activity is Na-24.

Reference [8] gives computed values of power density for 250 and 300 MWe sodium cooled reactors. Both have 45 cm thick radial blankets and 50 cm radial reflectors. Core power densities are 450 and 500 kW/l respectively. For both, gamma heating at the outer radial position in the reflector (90% stainless steel, 10% Na) is 0.030 $W/cm^3 = 0.004$ W/g. Normalizing to a more realistic core power density of 350 kW/l gives a heating rate of 0.003 W/g. But 1eV = 1.6E-19 W*sec. Hence the absorbed energy rate is 1.9E16 eV/g/sec for gammas from the core. This should be a reasonable approximation for gamma heating in most sodium-cooled fast reactors.

Saturated hydrocarbons, like ethane, generally have a molecular damage yield between 6 and 9 molecules/100 eV [9]. Conservatively setting G=10 molecules destroyed/100 eV, one can then combine that with the dose rate to find an ethane destruction rate of 1.9E15 molecules/g/sec. One gram of ethane contains N_{Av}/30.07=2E22 molecules/g. This yields a fractional destruction rate, f~1E-7 second^{-1}. Assuming 10% of ethane is in the IHX at any given time, the fractional rate becomes 1E-8 destructions/sec averaged over the PCS inventory. There are 3.16E7 seconds in a year, so in one year f=0.27; or 27% of the PCS inventory is depleted by radiolysis from the core, assuming no recombination.

The other main source of radiation is sodium, and the majority of radiation produced by sodium will come from Na-24, which has a half-life of around 15 hours. Sodium activity is almost entirely due to 15 hr-half life Na-24. A sodium-cooled fast reactor will have ~0.1 Ci/g of Na-24 (this is the Superphenix value, which is higher than other SFRs). Na-24 emits two gammas with total E = 4.2 MeV. At 3.7E10 decays per second/Ci this leads to 15.5E9 MeV/g/sec emitted and absorbed in a large pool of sodium. Assume that ethane and sodium have roughly the same energy absorption per gram. Once again using the conservative value of G=10 molecules destroyed/100 eV, one finds that the ethane destruction rate due to sodium is 1.55E15 molecules/g/sec. This means sodium activity could cause a fractional destruction rate of f=0.25 per year.

This is slightly misleading, however. A more realistic estimate can be gained by assuming that C_2H_6 has the same radiation absorption per gram of the IHX instead of per gram sodium. Roughly the fractions of each material in the IHX are:

Volume Fraction	Component	Density (g/cm^3)
0.25	C_2H_6	0.2
0.25	Na	1.0
0.5	steel	8.0

This yields an average IHX density of 4.3 g/cm^3. Therefore, per gram of IHX, the dose rate is about 1/4th as large as in pure sodium. And because the gamma absorption, $(\mu/\rho)_a$, varies slowly from element to element, the dose rate for C2H6 is roughly the same as that for the IHX as a whole [6]. The fractional destruction rate from Na-24 is therefore around 6% per year. When combined with the 27% per year from core radiation one gets a total of around 33%, which is tolerable, but suggests attention be paid to this issue, by addition of shielding and/or raising the IHX higher above the core.

2.8 Chapter Summary

Results were mixed about the thermal dissociation of ethane. Theoretical models predict that ethane should break down into methane and hydrogen, but current industrial practices show that ethane is effectively cracked into ethylene on a large-scale basis with only minor methane production. Also there is uncertainty surrounding rate constants. NIST does not have sufficient data to make judgments about rates of reactions, so the explanation might lie with the rates of reactions. Experimentation will be required to know definitively how ethane behaves in the high temperature/high pressure regime.

Radiolysis does not appear to be a significant issue, and the bulk of it can be reduced by simply moving heat exchangers farther from the core or adding additional shielding.

3. Reactions with Primary Coolants

3.1 Overview

In the event of a leak, it is important to know how primary and secondary loop coolants would interact. Of primary interest are interactions with sodium. The interaction between water and sodium is widely known, and much research is in progress on interactions between carbon dioxide and sodium since the resurgence in interest in supercritical CO_2 PCS systems. Ethane, though, is still an unknown. Reactions will also be considered between ethane and liquid salts as well as lead, since these are also coolant systems of current interest. These calculations are important to identify potential problems that may result from leaks, such as corrosive or potentially explosive products and excessive energy release.

3.2 Sodium

3.2.1 Sodium-H_2O Interaction

The reaction between sodium and water has been thoroughly researched and well-documented. It proceeds according to equations 3.1 and 3.2 when there is an excess of steam, and according to 3.2 when sodium is in abundance and temperature is above the melting point of NaOH.[16]

$$\text{Na (l)} + \text{H}_2\text{O (l)} \rightarrow \text{NaOH (s)} + 0.5\ \text{H}_2 + 147\ \text{kJ/mole} \tag{3.1}$$

$$\text{Na (l)} + \text{H}_2\text{O (g)} \rightarrow \text{NaOH (s)} + \text{H}_2 + 191\ \text{kJ/mole} \tag{3.2}$$

$$Na\ (l) + NaOH\ (l) \rightarrow Na_2O\ (s) + 0.5\ H_2 + 6.7\ \text{kJ/mole} \qquad (3.3)$$

Solid alkalis, such as sodium, react with water violently, and with liquid alkalis the reaction is even more violent. This creates engineering problems for operating the two systems in conjunction. Heat exchangers must be designed either with extra barriers, such as intermediate fluids, in place or that are able to withstand pressure and temperature spikes that could arise from a leak. Detectors must also be in place in order to identify small leaks. All of these steps sacrifice efficiency and safety. This reaction is especially dangerous because, in addition to being highly exothermic, it also produces large amounts of explosive hydrogen gas.

3.2.2 Sodium-CO_2 Interaction

The sodium-carbon dioxide reaction is also well researched. As early as the 1960s, experiments were being done to test the reactivity of carbon dioxide and liquid sodium [12]. Independent experiments and theoretical models have verified that equation 3.2 is the equation governing this reaction.

$$Na + 0.75\ CO_2 \rightarrow 0.5\ Na_2CO_3 + 0.25\ C + 271\ \text{kJ/mole} \qquad (3.4)$$

This reaction has been determined to be the result of equations 3.3 and 3.4.

$$Na + 0.25\ CO_2 \rightarrow 0.5\ Na_2O + 0.25\ C \qquad (3.5)$$

$$0.5\ Na_2O + 0.5\ CO_2 \rightarrow 0.5\ Na_2CO_3 \qquad (3.6)$$

Equation 3.5 represents the situation likely to be encountered in a heat exchanger leak; the high pressure CO_2 would be pushed into the primary system where there is an excess of sodium. Equation 3.5 is the rate limiting equation. Recent experiments have verified that liquid sodium and CO_2 react to give a significant amount of Na_2CO_3 and smaller amounts of solid carbon [13]. This study showed that the reaction proceeds readily at temperatures above 300°C and was very fast above 600°C. Conflicting studies place the temperature at which "rapid" reaction begins to occur between 450°C [12] and 600°C [14], but it is certain that at the temperatures involved in a LMFBR there would be a reaction.

HSC runs verified that theory matches experimental outcomes: the energy release is around 270 kJ/mol (fig 3.2), and if there is an excess of Na, there is less Na_2CO_3 produced and increasing amounts of carbon, as predicted by equation 3.7. Na_2CO_3 may, however, interact with sodium. Different reports give different theoretical answers [12], and there does not appear to be physical data, but it is possible that Na_2CO_3 reacts with sodium according to equation 3.7, to produce more carbon. Carbon in sodium can lead to carbonization of steel.

$$4\ Na + Na_2CO_3 \rightarrow 3\ Na_2O + C \tag{3.7}$$

While carbon dioxide does produce more energy than water when reacting with sodium, it has the advantage of not producing hydrogen. It also seems to proceed more slowly even though it releases more energy [12].

3.2.3 Sodium-Ethane Interaction

The sodium-ethane interaction was based upon equation 3.8. Similar to Eq. 3.5, it expresses the situation in which sodium is in abundance.

$$Na + 0.5\ C_2H_6 \rightarrow 0.5\ Na_2C_2 + 1.5\ H_2 \tag{3.8}$$

Evaluation was done using HSC from 773-873 K (500-600°C) at a pressure of 0.1 MPa. For completeness, all three coolants were tested.

In the temperature range considered all three coolants react. Note that ethane generates hydrogen gas, just like steam does and, unfortunately, makes more of it.

Figures 3.1 and 3.2 show the change in Gibbs free energy and enthalpy for sodium reacting with ethane, carbon dioxide and steam.

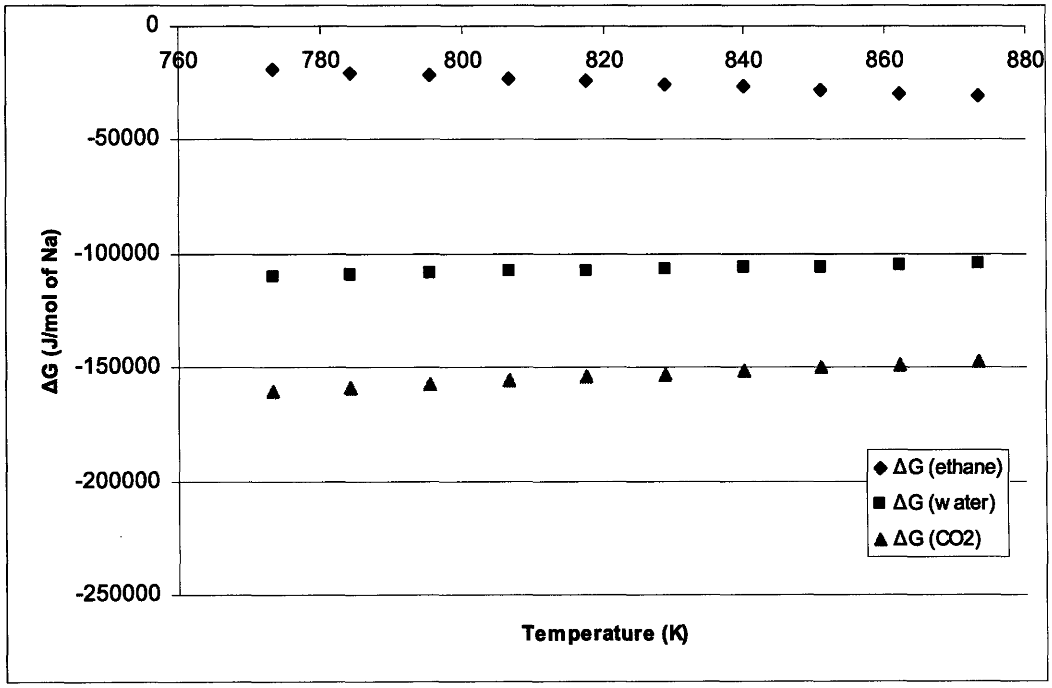

Figure 3.1: Reaction of Various Working Fluids and Sodium: Gibbs Free Energy Change per Mole of Na

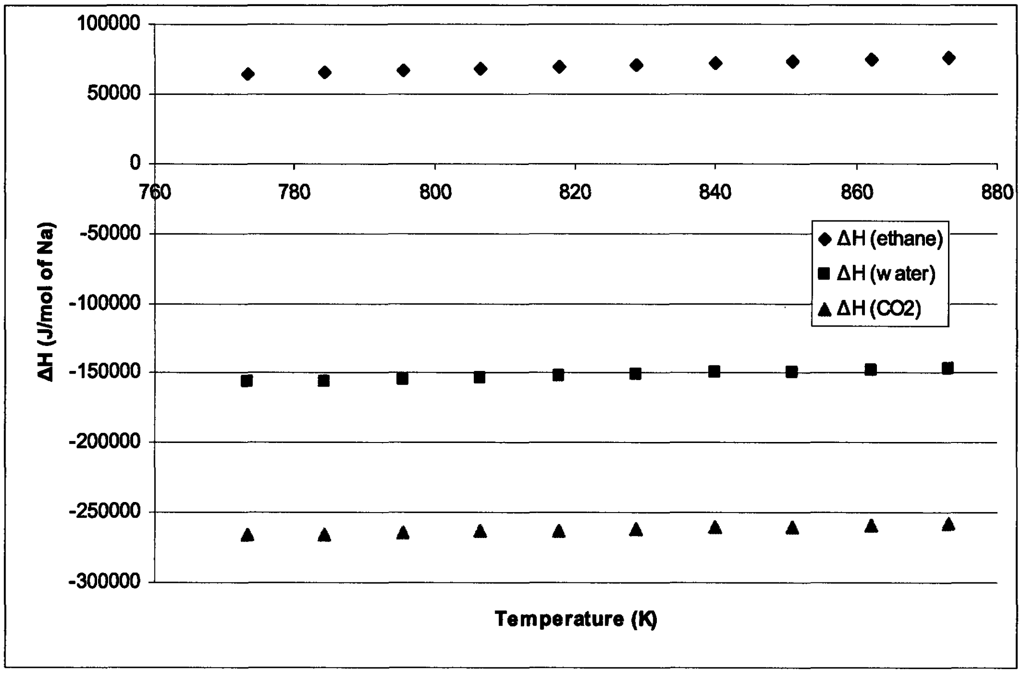

Figure 3.2: Reaction of Various Working Fluids and Sodium: Enthalpy Change per Mole of Na

Figure 3.1 shows that all three reactions have a negative change in Gibbs free energy, so all three will proceed spontaneously. Ethane does have the smallest magnitude, though, and it becomes less negative as temperature decreases. Thus, there is some temperature at which the reaction will stop going forward. Figure 3.2 differentiates ethane from the other options. The ethane-sodium reaction has a positive enthalpy change. This means that it will absorb energy, whereas the others give it off. These two facts taken in conjunction mean that an ethane sodium reaction could potentially be self quenching. At lower temperatures the enthalpy change for the reaction continues to drop, and around 573 K (300°C) it reaches zero and begins to go negative, hence becoming exothermic; see Figure 3.3.

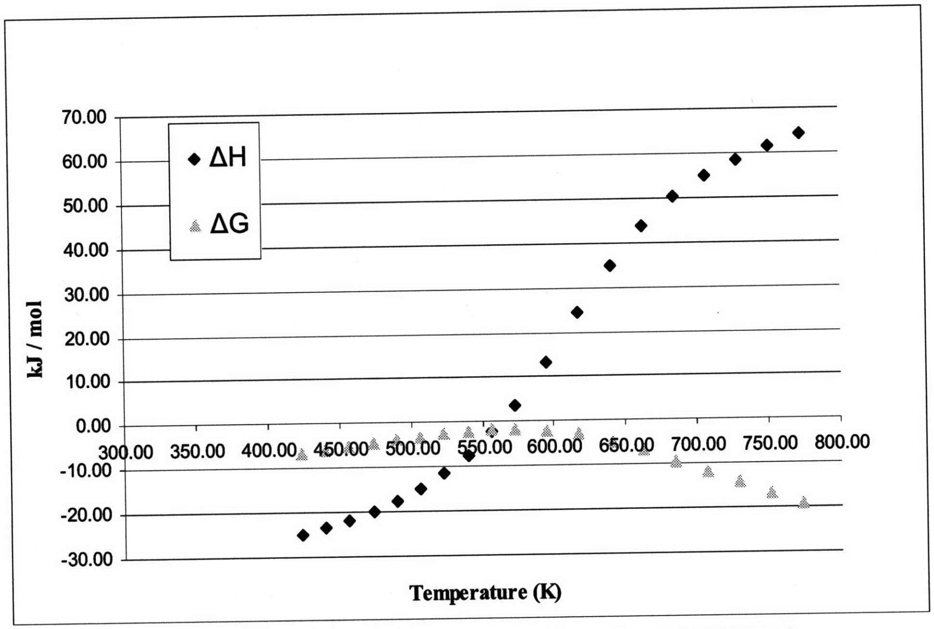

Figure 3.3 Energy/Enthalpy Change for Na Reaction (at 0.1 MPa)

The change in enthalpy for the sodium-ethane reaction (equation 3.6), is 75 kJ/mol-Na in the range of 500-600°C (773-873 K), and it steadily decreases at lower temperatures until it goes negative at 300°C (573 K). In order to look at the potential for a quenching reaction, consider a leak of 1 kg (33.3 moles) of ethane into the primary system. 33.3 moles of C_2H_6 react with 66.6 moles of Na.

$$66.6 \text{ mol}^* (75 \text{ kJ/mol}) = 5000\text{kJ absorbed}$$

$$C_{p,\,Na} = 32.7 \text{ J/mol}(^{\circ}C) \text{ [15]}$$

$$5000\text{kJ}/ C_p = 1.53\text{E}5 \text{ mol } (^{\circ}C) \text{ associated with 1 kg of } C_2H_6$$

If it were leaked slowly so that the energy absorption was spread evenly throughout the entire inventory of sodium (assuming 3000 tons of Na, which was the value for Superphenix), then 3E6 kg of sodium would be heated 0.001°C. If, however, the leak was faster and only 30 kg of sodium was cooled, by the same energy absorption, then it would experience a 100 degree drop. This though is an over-estimate because at 450°C the energy change is only 45 kJ/mol. This means that even in the case of an uncontained leak, sodium temperature would slowly drop and approach 300°C (which is well above sodium's melting point of 97.7°C). An ethane leak would also lead to production of hydrogen, but since temperature is in control, this should be an acceptable risk.

Another important factor is the speed of this reaction. Both steam and carbon dioxide are known to react quickly with sodium, and the quickness of this reaction can be part of the problem. Unfortunately NIST does not have information on the ethane-sodium interaction. Therefore, further experimentation will be necessary to identify how quickly the reaction proceeds.

Yevick claims that sodium will not react with hydrocarbons until they have been thermally decomposed. He says that sodium only reacts with the decomposition products, though he does not give any specific examples. If this is true then reaction rate would be dependant on rate of thermal dissociation. This serves only to reinforce the importance of thermal cracking experiments. [16]

3.3 Liquid Salts and Ethane

Ethane does not appear to react with liquid salts in the temperature range of interest. It was tested for reactions using NaCl, MgCl and NaF, which are all materials under current investigation. For all three salts tested, results were identical. As is shown in figure 3.4, large amounts of hydrogen gas and carbon are produced, and to a lesser extent, methane is as well. The amount of liquid salt remains constant. This means that there is no appreciable reaction between the liquid salts and the ethane, and what is witnessed are the products of ethane's thermal cracking. However, if ethane's thermal cracking is not apparent or is sufficiently slow, as was discussed in chapter 2, then it appears that ethane and liquid salts do not interact, making it a safe choice.

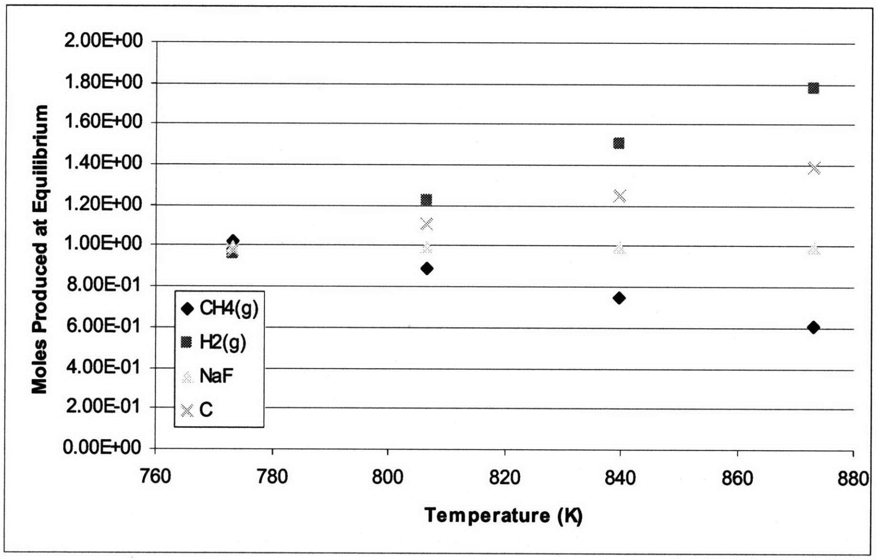

Figure 3.4: Equilibrium Products of Ethane-NaF Reaction

3.4 Lead and Ethane

Lead and lead-bismuth eutectic, in addition to sodium, are liquid metals under consideration as primary coolants. Like the liquid salts above, they do not react with ethane, but at the high temperatures of operation they do appear to contribute to the thermal dissociation of ethane. This means that if, somehow, this thermal cracking can be prevented or if it is a sufficiently slow reaction, ethane could be used with either of these systems.

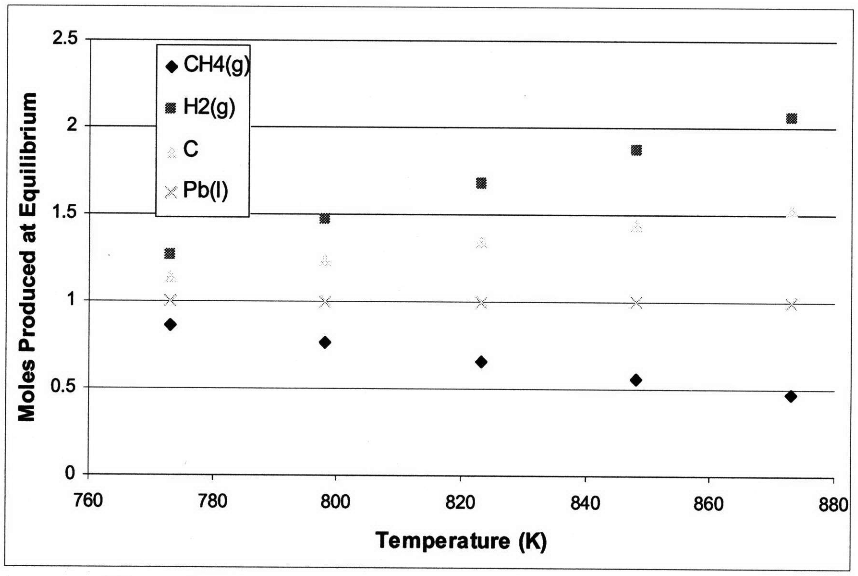

Figure 3.5: Equilibrium Products of Ethane-Pb Reaction

3.5 Chapter Summary

When compared with carbon dioxide or steam, ethane appears to be a worthwhile alternative. The ethane-sodium reaction is the only one of the three that is endothermic, which means that it has the potential to quench itself. Unfortunately, reaction rate data is unavailable, and this means that experimentation involving liquid sodium and gaseous ethane, similar to what has been done with CO_2 would be useful. Experimental data would verify energy absorption of the reaction as well as give valuable rate information. Tests should also be done to verify the claim that sodium only reacts with decomposition products of hydrocarbons. It should be relatively simple to test whether ethane alone reacts differently with sodium than ethane that has undergone a certain amount of thermal cracking.

Ethane, if it is thermally stable, appears to be inert in contact with liquid salts and lead. This reinforces the need for experimental verification of its behavior at high temperature and pressure, as discussed in chapter 2.

4. Component and Cost Scaling

4.1 Chapter Introduction

Aside from all considerations of thermal viability, there is another issue which is of paramount importance: efficiency. If ethane does not have the potential to provide an equivalent or higher efficiency cycle compared to CO_2, then further inquiry and experimentation would be wasted. Therefore it is important to provide a basis for belief in competitive efficiency.

Table 4.1 compares various chemical and thermodynamic properties of ethane and carbon dioxide. The similarity of critical temperatures is an indication that ethane can perform comparably to carbon dioxide because of the law of corresponding states. Also of interest are the heat capacity, thermal conductivity, and critical pressure. Higher heat capacity and thermal conductivity imply improved performance. Lower critical pressure means that an optimized ethane system should be easier to build, as walls may not have to be as thick. Lower critical density means higher compressor work per unit mass flow rate, but it also means a higher tolerable mass flow that should offset this constraint.

Table 4.1: Thermodynamic Properties of CO_2 and Ethane

	CO_2	C_2H_6	Ratio $\frac{C_2H_6}{CO_2}$
Molecular Mass, M	44.01	30.07	0.683
Critical Pressure (MPa)	7.377	4.89	0.663
Critical Temperature (°C)	31	32.2	1.039
Critical Density, ρ_c (kg/m^3)	497.6	203	0.408
Heat Capacity, C_p (kJ/kg*°C) †	1.2	3.79	3.158
Viscosity, μ (kg/m*s) †	3.60E-05	2.50E-05	0.694
Density (kg/m^3) (ideal gas)†	0.606	0.414	0.683
Thermal Conductivity, k (W/m*°C) †	0.06	0.132	2.200
γ (C_p/C_v)	1.2	1.1	0.917
$Pr = C_p*\mu/k$	0.73	0.72	0.986

†- at 600°C, 1 atm

4.2 IHX Scaling

Table 4.2 summarizes indices related to heat exchanger design. These indices come from Appendix A of J. I. Shin's work [17]. He makes several basic assumptions in creating them: temperature change across all heat transfer boundaries and through all heat exchangers is constant (in order to maintain comparable thermodynamic efficiency), the ratio of pumping power to energy transfer is held constant, gases are assumed to be ideal and have constant Prandtl number, and fixed system pressure. He considers two variations: constant channel length with varying diameter and constant diameter with varying channel length. Both cases are presented below in Table 4.2. These relations are intended only for a primary comparison. They represent non-optimized systems under a host of constraints, but they should be sufficient to give an indication of relative sizes.

Table 4.2 shows that there are some striking attributes of ethane. Its higher Reynold's number and heat transfer coefficient translate into much smaller heat exchangers – by up to a factor of three. Since these ratios do not include any kind of optimization, this means a more efficient and less expensive ethane system is possible and more research is therefore encouraged.

Table 4.2: Heat Exchanger Scaling

	Fixed Length, Varying Diameter		Fixed Diameter, Varying Length	
	Relation	Ratio C_2H_6 CO_2	Relation	Ratio C_2H_6 CO_2
Channel Velocity	$C_p^{1/2}$	1.78	$C_p^{1/2}$	1.78
Number of Channels	$M^{-2/3}Cp^{-4/3}\,\mu^{-1/3}$	0.31	$M^{-1}C_p^{-3/2}$	0.261
Channel Surface Area (total)	$M^{-5/6}C_p^{-17/12}\,\mu^{-1/6}$	0.29	$M^{-4/5}C_p^{-7/5}\,\mu^{-1/5}$	0.292
Channel Diameter	$M^{-1/6}C_p^{-1/12}\,\mu^{-1/6}$	1.03	-----	-----
	$M^{-1}C_p^{-3/2}$	0.26	-----	-----
Channel Length	-----	-----	$M^{-1/5}C_p^{-1/10}\,\mu^{-1/5}$	1.04
Duct Diameter	$M^{-5/12}C_p^{-7/12}\,\mu^{1/24}$	0.59	$M^{-5/12}C_p^{-7/12}\,\mu^{1/24}$	0.59

4.3 Turbomachinery Scaling

Turbomachinery scaling ratios come from the same source [17], and are important because often the same working fluid properties will have opposite effects on the two systems. Again there are some basic assumptions that go into them. Table 4.3 compares design parameters for turbomachinery scaling. Ethane's low gas bending stress is advantageous, but the number of stages is a severe drawback. If ethane requires 3-5 times as many stages as carbon dioxide, then its turbomachinery could be more expensive. Even helium and steam only require around twice as many stages.

Table 4.3: Turbomachinery Scaling

	Dependence	Ratio $\frac{C_2H_6}{CO_2}$
Diameter	$(1/MC_p)^{1/3}$	0.774
Mass Flow Rate (kg/s)	$1/C_p$	0.317
Volumetric Flow Rate (m3/s)	$1/(MC_p)$	0.463
Number of Stages	$(MC_p)2/3*C_p$	5.27
	C_p	3.16
Flow Velocity (m/s)	$(1/MC_p)^{1/3}$	0.774
Speed of Sound, m	$M^{-1/2}$	1.21
Mach Number	$M^{1/2}$	0.827
Gas Bending Stress, ksi	$1/(C_p{}^2*(MC_p))$	0.046
Reynolds Number	$1/(\mu*(MC_p)^{2/3})$	0.862
	m / ρ_c	0.74

4.4 Size Comparison

Another important factor in the comparison between ethane and carbon dioxide PCSs is their relative cost. According to Freas' thesis, 87,000 kg of CO2 must be kept on site to accommodate a 300 MW_e plant. 58,000 kg are needed for the PCS inventory itself, and an additional 50% is needed in case of leaks. This would provide leakage make-up for 100 days assuming a 0.5% per day leak rate. [18]

This means that in order to maintain the same number of moles of gas:

$$(30/44) * 87,000 = 59,320 \text{ kg of C2H6}$$

~60,000 kg of C2H6 are needed. This is roughly 200 kg/MWe.

4.5 Chapter Summary

All of the results in this chapter are subject to optimization, and it is not immediately clear which effects are strongest. The IHX is predicted to be more efficient with ethane, but the turbomachinery appears to require more stages. Reduced flow rate also means that it should have smaller diameter, and reduced size might help to offset an increase in stages. Numerous further analyses are needed for a more complete understanding of the system, including a better understanding of how ethane behaves at higher temperature and pressure. The prospects appear attractive and thus, more examination is recommended.

5. Conclusions and Recommendations

An ethane-based Brayton power conversion system deserves further research. Computer simulations give mixed results, but ethylene industry experience suggests that use in a power conversion system may still be possible. Limited rate data also suggests that recombination should be much faster than dissociation, which could reconstitute pure ethylene at compression inlet conditions (35°C, 8 MPa). The next step should be to run experiments to verify ethane's behavior at high temperature and pressure and verify whether it will dissociate excessively. Even if it does, the rate and extent of recombination at lower temperatures should be evaluated. If stability up to about 300°C can be confirmed, then ethane can be employed for geothermal applications even if higher temperature service proves impracticable. [19]

A simple experiment in which ethane is heated in a fixed volume flask and pressure is measured as a function of temperature and time is proposed. If dissociation occurs then the pressure will increase. Using the ideal gas law: $PV=nRT$ one can establish a molecular dissociation ratio, r, comparing results to standard conditions:

$$r = (n/n_0) = (P/P_0) * (T_0/T)$$

If this ratio rises then dissociation is occurring, but if it drops back to 1.0 the products are recombining. If this test is successful, then more elaborate loop experiments can be designed.

If ethane is determined to be sufficiently thermally stable, then experiments should be run to test its reactivity with liquid sodium. Also cycle performance calculations should be carried out under optimized conditions to compare the efficiency of ethane and CO_2 cycles.

References:

[1] V. Dostal, M.J. Driscoll, P. Hejzlar. "High Performance Supercritical Carbon Dioxide Cycle for Next Generation Nuclear Reactors," Nuclear Technology, Vol. 154, No. 3, June 2006.

[2] G.E. Apostolakis et al. "Risk-Informed Balancing of Safety, Non-Proliferation, and Economics for the Sodium Cooled Fast Reactor (SFR), NERI Project No. 08-020.

[3] A. Roine. Outokumpu HSC Chemistry for Windows: Chemical Reaction and Equilibrium Software with Extensive Thermodynamical Database, Version 5.1., User's Guide. 02103-ORC-T, Outokumpu Research Oy, Finland, 2002.

[4] H. Zimmermann, R. Walzi. Ullman's Encyclopedia of Industrial Chemistry. Wiley-VCH Verlag GmbH & Co., 2007. http://www.mrw.interscience.wiley.com/emrw/9783527306732/ueic/article/a10_045/current/html?hd=All%2Cethylene

[5] S. Raseev. Thermal and Catalytic Processes in Petroleum Refining. Marcel Dekker, 2003.

[6] Etherington, Harold. Nuclear Engineering Handbook. McGraw-Hill, 1958.

[7] Handbook of Compressed Gas 3rd Edition, Compressed Gas Association, 1990.

[8] M.S. Kalra and M. J. Driscoll "Gamma Heating in LMFBR Media" MITNE-179, Feb. 1976, pp. 105, 108, 175.

[9] Robert Bolt, James Carroll, "Radiation Effects on Organic Materials" Academic Press, 1963. pp. 55, 71, 117.

[10] A. Trenwith. "Re-examination of the Thermal Dissociation of Ethane." Thesis, Dept. of Inorganic Chemistry, School of Chemistry, The University, Newcastle upon Tyne, 1978.

[11] M. C. Lin and M. H. Black. "The Thermal Decomposition of Ethane." Dept. of Chemistry Thesis, University of Ottawa, 1996.

[12] C. Latge, G. Rodriguez, N. Simon, "Supercritical CO2 Brayton Cycle for SFR: Na-CO2 interaction and consequences on design and operation." Global, 2005.

[13] J.H. Choi, S.D. Suk, D. Choi, J.M. Kim, D. Hahn, J. H. Cahalan, "Capsule Test for Investigating the Sodium-Carbon Dioxide Interaction." ICAPP '06, Paper 6369.

[14] H. Ishikawa, S. Miyahara, Y. Yoshizawa, "Experimental Study of Sodium – Carbon Dioxide Reaction." Paper 5688, ICAPP '05.

[15] V.E. Zinovev. "Handbook of Thermophysical Properties of Metals at High Temperatures" Nova Science Publications, 1996.

[16] J. Yevick, A. Amorosi. "Fast Reactor Technology: Plant Design" The MIT Press, 1966.

[17] Shin, J. I. "Conceptual Design of an HTGR System for a Total Energy Application," Appendix A. Nuclear Engineering Thesis, MIT, 1975.

[18] Freas, R. "Analysis of Required Supporting Systems for the Supercritical CO_2 Power Conversion System," Nuclear Engineering Thesis, MIT, 2003.

[19] "The Future of Geothermal Energy" Interdisciplinary Report, MIT, 2006.

http://www1.eere.energy.gov/geothermal/egx_technology.html

Appendix A: Data in Support of Figures

This appendix provides the numerical data for all plots derived from the HSC® code. A full description of this code can be found in section 1.4 of this report. Because temperature parameters for runs are entered in Celsius and output is in Kelvin, most input temperatures are cited as round numbers in Celsius and not Kelvin.

A.2.0 – Comparison of Ethane Cracking at High and Low Pressures

This data comes from an HSC run analyzing Equation 2.1. It is similar to figures 2.1 and 2.3 except it also includes a data set at the low pressure at which industrial ethane cracking occurs. It is present to verify the stipulated assumption that at high temperature and low pressure ethane fully dissociates into ethylene. It also effectively illustrates the difference that pressure makes on the reaction.

T (K)	Dissociation Fraction (1 bar)	Dissociation Fraction (200 bar)
423.15	5.12E-06	3.62E-07
462.624	2.78E-05	1.97E-06
502.097	1.16E-04	8.24E-06
541.571	3.98E-04	2.81E-05
581.045	1.15E-03	8.15E-05
620.518	2.93E-03	2.07E-04
659.992	6.67E-03	4.72E-04
699.466	1.39E-02	9.81E-04
738.939	2.67E-02	1.89E-03
778.413	4.81E-02	3.41E-03
817.887	8.19E-02	5.81E-03
857.361	1.32E-01	9.44E-03
896.834	2.04E-01	1.47E-02
936.308	2.98E-01	2.21E-02
975.782	4.13E-01	3.21E-02
1015.255	5.39E-01	4.52E-02
1054.729	6.61E-01	6.22E-02
1094.203	7.64E-01	8.35E-02
1133.676	8.42E-01	1.10E-01
1173.15	8.96E-01	1.41E-01

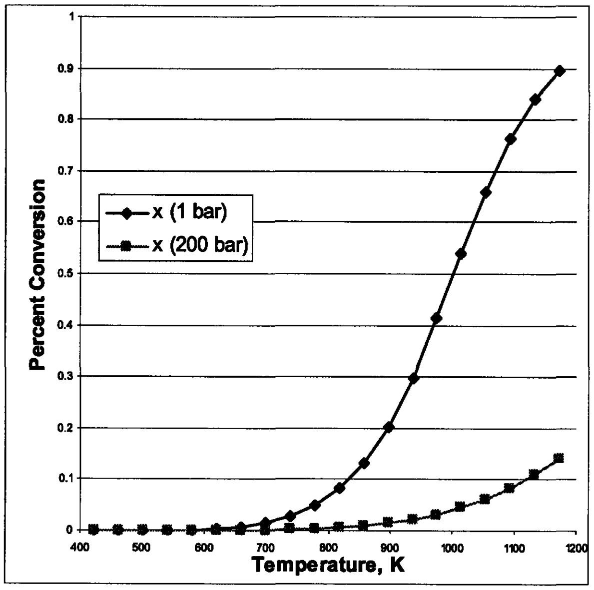

A.2.1 - Figure 2.1: Fraction of Ethane Cracking vs. 1/Temperature

Figure 2.1 is a plot of the amount of ethane cracking as a function of inverse temperature. The program started with 1 mol of ethane (C_2H_6) and considered the reaction that would turn it into ethylene (C_2H_4) and hydrogen gas. The run was performed at a constant pressure of 20 MPa varying temperature from 150-650°C (423-923 K).

Temperature (K)	1/Temp (K^{-1})	Fraction of Ethane Converted
423.15	0.002363	3.62E-07
468.605	0.002134	2.48E-06
514.059	0.001945	1.22E-05
559.514	0.001787	4.65E-05
604.968	0.001653	1.46E-04
650.423	0.001537	3.90E-04
695.877	0.001437	9.21E-04
741.332	0.001349	1.96E-03
786.786	0.001271	3.83E-03
832.241	0.001202	6.97E-03
877.695	0.001139	1.19E-02
923.15	0.001083	1.93E-02

A.2.2 - Figure 2.2: Fraction of Ethane Cracking vs. Pressure

Figure 2.2 is similar to 2.1 except it has a variable pressure (0.1-20 MPa) and a constant temperature of 550°C.

Pressure (MPa)	Fraction of Ethane Converted
0.1	8.75E-02
1.095	2.65E-02
2.09	1.92E-02
3.085	1.58E-02
4.08	1.38E-02
5.075	1.23E-02
6.07	1.13E-02
7.065	1.05E-02
8.06	9.79E-03
9.055	9.23E-03
10.05	8.77E-03
11.045	8.36E-03
12.04	8.01E-03
13.035	7.70E-03
14.03	7.42E-03
15.025	7.17E-03
16.02	6.94E-03
17.015	6.74E-03
18.01	6.55E-03
19.005	6.37E-03
20	6.21E-03

A.2.3 - Figure 2.3: Decomposition of 1 mol of Ethane vs. Temp (K)

Each column represents the number of moles of that compound produced from 1 mole of ethane (C_2H_6) at the indicated temperature and a pressure of 20 MPa. Ethane, methane (CH_4), and ethylene (C_2H_4), as expected, are the primary components. Other, lighter hydrocarbons are included for completeness, and are several orders of magnitude less prevalent. For practical purposes, only the three compounds listed above are considered.

Temp (K)	CH_2(g)	Methane $CH_4(g)^*$	C_2H_2(g)	Ethylene $C_2H_4(g)^*$	C_2H_5(g)	Ethane $C_2H_6(g)^*$	H(g)	H_2(g)
298.15	4.99E-62	2.56E-03	1.41E-13	1.28E-03	2.19E-22	9.97E-01	4.66E-46	7.30E-18
353.706	8.95E-52	1.18E-02	3.43E-11	5.92E-03	1.14E-18	9.88E-01	1.71E-38	9.59E-15
409.262	2.72E-44	3.60E-02	1.95E-09	1.80E-02	5.76E-16	9.64E-01	5.75E-33	1.87E-12
464.818	1.36E-38	8.28E-02	4.30E-08	4.14E-02	6.38E-14	9.17E-01	9.56E-29	1.06E-10
520.374	4.17E-34	1.56E-01	4.96E-07	7.78E-02	2.49E-12	8.44E-01	2.05E-25	2.59E-09
575.93	1.74E-30	2.51E-01	3.58E-06	1.26E-01	4.58E-11	7.49E-01	1.02E-22	3.44E-08
631.486	1.65E-27	3.60E-01	1.81E-05	1.80E-01	4.80E-10	6.40E-01	1.73E-20	2.90E-07
687.042	5.12E-25	4.69E-01	6.95E-05	2.35E-01	3.28E-09	5.31E-01	1.28E-18	1.72E-06
742.598	6.62E-23	5.69E-01	2.15E-04	2.84E-01	1.61E-08	4.31E-01	5.00E-17	7.78E-06
798.154	4.28E-21	6.54E-01	5.62E-04	3.26E-01	6.10E-08	3.46E-01	1.17E-15	2.83E-05

A.2.4 - Figure 2.4: Time Constants for Ethane Cracking Reaction

Data in each set are segmented according the separate data sets from which they were gleaned. NIST gives equations for k(T) over a specific temperature range. High and low temperatures for each represent limits for which equations are applicable, and others are distributed evenly within. All second order values, as well as data set (1) come from "extensive literature review." (2) comes from Vis-UV absorption at 1 atm, and (3) comes from Calculated – RRK(M) extrapolation. The aberrant data set (lower than the other two) for the second order is (6).

First Order

T (K)	k (sec^{-1})	
300	1.06E-48	(1)
512.5	1.48E-21	
725	2.15E-10	
937.5	0.000251	
1150	1.59147	
1362.5	634.1279	
1575	48920.11	
1787.5	1316445	
2000	17323785	
1350	47.45408	(2)
1540	1008.249	
1730	8619.504	
1920	39784.62	
2110	119151.7	
843	4.25E-07	(3)
1079.714	0.040982	
1316.429	59.36683	
1553.143	8903.395	
1789.857	342190.3	
2026.571	5454187	
2263.286	47659065	
2500	2.71E+08	

Second Order

	T (K)	k (cc/mol/sec)
(4)	300	2.79E-64
	583.3333	1.53E-33
	866.6667	1.7E-23
	1150	1.08E-18
	1433.333	5.78E-16
	1716.667	2.97E-14
	2000	4.11E-13
(5)	300	1.74E-40
	583.3333	9.38E-10
	866.6667	10.39887
	1150	658484.9
	1433.333	3.51E+08
	1716.667	1.8E+10
	2000	2.49E+11
(6)	800	2.463583
	1140	873877.7
	1480	8.74E+08
	1820	6.61E+10
	2160	1.28E+12
	2500	1.11E+13

Specific equations used to generate data and reference sources are below:

(1) 94BAU/COB - Baulch,D.L.; Cobos,C.J.; Cox,R.A.; Frank,P.; Hayman,G.; Just,Th.; Kerr,J.A.; Murrells,T.; Pilling,M.J.; Troe,J.; Walker,R.W.; Warnatz,J.
Evaluated kinetic data for combustion modeling. Supplement I

k(T)=1.54e18*(T/298)^(-1.24)*(EXP(-45700/T))

(2) 93DAV/DIR - Davidson,D.F.; DiRosa,M.D.; Hanson,R.K.; Bowman,C.T.
A study of ethane decomposition in a shock tube using laser absorption of CH3

k(T)=1.38E+32*(T/298)^(-17.6)*EXP(-58800/T)

(3) 89TSA - Tsang,W. Rate constants for the decomposition and formation of simple alkanes over extended temperature and pressure ranges

k(T)=1.12E18*(T/298)^(-1.79)*EXP(-45834/T)

(4) 94BAU/COB - Baulch,D.L.; Cobos,C.J.; Cox,R.A.; Frank,P.; Hayman,G.; Just,Th.; Kerr,J.A.; Murrells,T.; Pilling,M.J.; Troe,J.; Walker,R.W.; Warnatz,J.
Evaluated kinetic data for combustion modelling. Supplement I

k(T)=45100*(T/298)^(-8.24)*EXP(-47100/T)

(5) 94BAU/COB - Baulch,D.L.; Cobos,C.J.; Cox,R.A.; Frank,P.; Hayman,G.; Just,Th.; Kerr,J.A.; Murrells,T.; Pilling,M.J.; Troe,J.; Walker,R.W.; Warnatz,J.
Evaluated kinetic data for combustion modelling. Supplement I

k(T)=2.72E28*(T/298)^(-8.24)*EXP(-47090/T)

(6) 84WAR - Warnatz, J. Rate coefficients in the C/H/O system

k(T)=1e19*EXP(-34278/T)

A.2.5 Figure 2.5: Experimental and Theoretical Time Constants For the Dissociation of Ethane

The bulk of the data for Figure 2.5 is repeated from 2.4: specifically data sets (4), (5), and (6). The two new sets of data come from experimental sources and are presented specifically to illustrate the uncertainty that arises from the expected values and especially resulting from pressure variation.

T (K)	k (cc/mol/sec)
913	8051.786
934.5	20191.06
956	48581.09
977.5	112460.9
999	251099.3

This is the upper set of new data in the figure. It was acquired via gas chromatography at a pressure between 1.34E-4 and 2.66E-2 MPa in a static or low flow. Source information is as follows:

66LIN/BAC2 - Lin,M.C.; Back,M.H. The thermal decomposition of ethane. Part II. The unimolecular decomposition of the ethane molecule and the ethyl radical
Can. J. Chem. 44, 2357 (1966)

k(T)=1.82E21*EXP(-36483/T)

T (K)	k (cc/mol/sec)
1043	0.000658
1103	0.005659
1163	0.03899

This is the lower set of new data in the figure. It was also acquired via gas chromatography but at a pressure of 0.1 MPa in a static or low flow. Source information is as follows:

60BRO/KAL - Brodsky, A.M.; Kalinenko, R.A.; Lavrovsky, K.P. The principles governing high-temperature ethane cracking J. Chem. Soc., 4443 (1960)

k(T)=1E14*EXP(-41264/T)

A.2.6 – Figure 2.6: Experimentally-Derived Rate Constants for Ethylene Production

Figure 2.6 shows what data the NIST database has on the reaction:

$$C_2H_6 \rightarrow C_2H_4 + H_2$$

Unfortunately NIST only has four data sets that cover relatively small temperature ranges.

First Order

T (K)	k	
873	0.000337	(1)
873	0.00067216	(2)
973	0.0509971	

Second Order

	T (K)	k
(3)	1043	0.453883
	1073	1.371931
	1103	3.904715
	1133	10.51454
	1163	26.90277
(4)	1800	1.4E+09
	1975	7.5E+09
	2150	3.05E+10
	2325	1E+11
	2500	2.8E+11

Format for analysis is similar to what is described in A.2.4. All first order data were taken directly and second order were taken via gas chromatography. All were done at low or static flow.

Specific equations used to generate data and reference sources are below:

(1) 55SIL - Silcocks,C.G., The kinetics of the thermal decomposition and polymerization of ethane and ethylene. Proc. R. Soc. London A: 233, 465-479 (1955)

k(T=873 K)=0.000337

(2) 31MAR/MCC - Marek,L.F.; McCluer,W.B., Velocity constants ofr the thermal dissociation of ethane and propane. Ind. Eng. Chem. 23, 878-881 (1931)

k(T)=1.32E15*EXP(-36772/T)

(3) 60BRO/KAL - Brodsky, A.M.; Kalinenko, R.A.; Lavrovsky, K.P., The principles governing high-temperature ethane cracking J. Chem. Soc. , 4443 (1960)

k(T)=6.9E16*EXP(-41264/T)

(4) 856SCH/KLO - Schulz, G.; Klotz, H.-D.; Spangenberg, H.-J., Reaktionsmodell zur bruttokinetik der pyrolyse von methan im stosswellenrohr bei temperaturen von 1800 K bis 2500 K. Z. Chem. 25, 88 (1985)

k(T)=2.29E17*EXP(-34039/T)

A.2.7 – Thermal Dissociation of Carbon Dioxide and Water

The data below are from an HSC calculation looking at the thermal dissociation of CO_2 at a constant pressure of 1 bar. The same calculation at 200 bar yielded the same results.

T (K)	373.15	439.817	506.484	573.151	639.818
C_2(g)	1.98E-128	3.06E-55	1.89E-53	1.59E-52	1.04E-97
C_3(g)	2.07E-134	3.48E-54	1.48E-53	2.77E-52	2.62E-55
C_4(g)	1.81E-166	6.89E-53	2.96E-55	1.90E-54	8.54E-60
C_5(g)	6.74E-47	5.48E-57	2.16E-55	1.26E-54	7.86E-60
C60(g)	7.42E-43	2.71E-51	2.59E-52	3.14E-50	6.92E-56
CO(g)	2.88E-13	9.52E-13	9.69E-13	1.05E-12	8.55E-13
CO_2(g)	**1.00E+00**	**1.00E+00**	**1.00E+00**	**1.00E+00**	**1.00E+00**
C_2O(g)	1.91E-77	2.91E-50	4.37E-46	2.80E-45	6.40E-63
C_3O_2(g)	2.50E-60	1.82E-42	8.59E-42	8.09E-41	3.99E-61
O(g)	4.34E-55	2.72E-44	5.93E-36	1.41E-29	2.06E-24
O_2(g)	8.11E-46	7.91E-35	5.61E-26	3.06E-19	1.12E-13
O_3(g)	8.32E-92	4.11E-57	1.11E-49	1.37E-45	2.45E-35

T (K)	706.485	773.152	839.819	906.486	973.153
C_2(g)	7.73E-89	7.49E-81	3.92E-74	2.12E-68	1.88E-63
C_3(g)	4.14E-104	5.93E-95	2.98E-87	1.10E-80	5.15E-75
C_4(g)	4.26E-134	1.17E-122	4.95E-113	8.08E-105	9.93E-98
C_5(g)	2.85E-152	1.89E-139	1.16E-128	1.88E-119	1.68E-111
C60(g)	1.00E-300	1.00E-300	1.00E-300	1.00E-300	1.00E-300
CO(g)	1.56E-11	2.50E-10	2.58E-09	1.88E-08	1.04E-07
CO_2(g)	**1.00E+00**	**1.00E+00**	**1.00E+00**	**1.00E+00**	**1.00E+00**
C_2O(g)	2.15E-57	2.45E-52	4.41E-48	1.89E-44	2.57E-41
C_3O_2(g)	2.00E-56	6.83E-52	4.46E-48	8.02E-45	5.18E-42
O(g)	1.49E-21	2.40E-19	1.73E-17	6.64E-16	1.55E-14
O_2(g)	7.82E-12	1.25E-10	1.29E-09	9.40E-09	5.22E-08
O_3(g)	1.77E-31	9.11E-29	1.74E-26	1.54E-24	7.37E-23

The data below are results showing that water does not thermally dissociate at higher temperatures. It was run at pressure of 1 bar.

T (K)	473.15	573.15	673.15	773.15	873.15	973.15	1073.15
H(g)	4.32E-31	1.59E-24	2.29E-20	2.50E-17	5.56E-15	4.13E-13	1.39E-11
H2(g)	1.53E-18	7.31E-14	1.67E-11	7.37E-10	1.38E-08	1.42E-07	9.58E-07
HO2(g)	4.30E-25	1.05E-22	1.29E-19	3.73E-17	2.96E-15	9.62E-14	1.64E-12
H2O(g)	**1.00E+00**	**1.00E+00**	**1.00E+00**	**1.00E+00**	**1.00E+00**	**1.00E+00**	**1.00E+00**
H2O2(g)	6.31E-22	7.04E-20	1.70E-17	1.29E-15	3.67E-14	5.28E-13	4.65E-12
O(g)	1.16E-31	8.15E-27	1.85E-22	4.10E-19	1.58E-16	1.80E-14	8.52E-13
O2(g)	9.41E-14	1.02E-13	8.33E-12	3.66E-10	6.82E-09	6.99E-08	4.66E-07
O3(g)	1.60E-39	9.66E-37	5.88E-32	4.56E-28	4.62E-25	1.14E-22	1.02E-20
OH(g)	1.16E-19	1.51E-16	7.02E-14	7.64E-12	2.85E-10	5.09E-09	5.31E-08
H2O	0.00E+00	0.00E+00	0.00E+00	0.00E+00	0.00E+00	0.00E+00	0.00E+00
H2O(l)	0.00E+00	0.00E+00	0.00E+00	0.00E+00	0.00E+00	0.00E+00	0.00E+00
H2O2(l)	0.00E+00	0.00E+00	0.00E+00	0.00E+00	0.00E+00	0.00E+00	0.00E+00

A.3.1 - Figure 3.1: Reaction of Various Coolants and Sodium: Gibbs Free Energy Change per Mole of Na

Reactions were computed at 0.1 MPa according to equations 3.1, 3.2 and 3.5.

Temperature (K)	ΔG C_2H_6 (kJ/mol-Na)	ΔG H_2O (kJ/mol-Na)	ΔG CO_2 (kJ/mol-Na)
773.15	-19.2002	-109.824	-160.456
784.261	-20.4334	-109.174	-158.897
795.372	-21.7244	-108.531	-157.363
806.483	-22.9826	-107.903	-155.935
817.594	-24.2145	-107.298	-154.351
828.706	-25.5628	-106.698	-152.891
839.817	-26.8725	-106.12	-151.456
850.928	-28.2055	-105.554	-149.945
862.039	-29.4957	-105	-148.645
873.15	-30.9043	-104.366	-147.185

A.3.2 - Figure 3.2: Reaction of Various Coolants and Sodium: Enthalpy Change per Mole of Na

Both enthalpy and entropy results are given because entropy (as well as Gibbs energy) is explicitly given in the HSC code, and enthalpy is derived from these values. Data for lower temperatures is available more fully below.

Temperature (K)	ΔH C_2H_6 (kJ/mol-Na)	ΔH H_2O (kJ/mol-Na)	ΔH CO_2 (kJ/mol-Na)
773.15	64.3	-156.6	-266.3
784.261	65.6	-155.5	-265.4
795.372	66.88	-154.4	-264.5
806.483	68.15	-153.3	-263.6
817.594	69.4	-152.2	-262.6
828.706	70.65	-151.1	-261.7
839.817	71.89	-150	-260.8
850.928	73.14	-148.9	-259.8
862.039	74.38	-147.8	-258.9
873.15	75.62	-146.6	-257.9

Temperature (K)	ΔS C_2H_6 (J/K mol-Na)	ΔS H_2O (J/K mol-Na)	ΔS CO_2 (J/K mol-Na)
773.15	108	-60.5	-136.9
784.261	109.7	-59.07	-135.8
795.372	111.4	-57.67	-134.7
806.483	113	-56.29	-133.5
817.594	114.5	-54.92	-132.4
828.706	116.1	-53.58	-131.3
839.817	117.6	-52.25	-130.2
850.928	119.1	-50.94	-129.1
862.039	120.5	-49.65	-127.9
873.15	122	-48.37	-126.8

A.3.3 - Figure 3.3 Energy/Enthalpy Change for Na-C_2H_6 Reaction (at 0.1 MPa)

Temperature (K)	ΔH (kJ/mol-Na)	ΔG (kJ/mol-Na)
423.15	-25.06	-6.98726
439.82	-23.51	-6.18121
456.48	-21.77	-5.40048
473.15	-19.78	-4.6439
489.82	-17.48	-3.93653
506.49	-14.77	-3.27279
523.15	-11.54	-2.67781
539.82	-7.65	-2.17724
556.49	-2.36	-1.82961
573.15	3.64	-1.70
595.37	13.31	-2.01
617.59	24.28	-3.04
639.82	34.96	-4.79
662.04	43.76	-7.01
684.26	50.23	-9.42
706.48	54.92	-11.86
728.70	58.53	-14.30
750.93	61.56	-16.76
773.15	64.30	-19.20

A.3.4 - Figure 3.4: Equilibrium Products of Ethane-NaF Reaction

Starred compounds (CH_4^*, H_2^*, NaF^*, C^*) are the only ones included in Figure 3.4. All others were present in such small quantities to make them indistinguishable on a graph.

T (K)	773.15	806.483	839.817	873.15
$CH(g)$	7.83E-35	4.16E-33	1.60E-31	4.60E-30
$CH_2(g)$	5.94E-24	8.85E-23	1.04E-21	9.98E-21
$CH_3(g)$	2.02E-11	6.90E-11	2.08E-10	5.56E-10
$CH_4(g)^*$	**1.02E+00**	**8.87E-01**	**7.49E-01**	**6.12E-01**
$C_2H(g)$	5.83E-26	1.45E-24	2.78E-23	4.20E-22
$C_2H_2(g)$	4.41E-13	2.39E-12	1.11E-11	4.50E-11
$C_2H_3(g)$	1.73E-17	1.21E-16	7.01E-16	3.44E-15
$C_2H_4(g)$	7.17E-08	1.42E-07	2.54E-07	4.16E-07
$C_2H_5(g)$	1.12E-13	3.35E-13	8.66E-13	1.97E-12
$C_2H_6(g)$	1.75E-05	1.64E-05	1.45E-05	1.21E-05
$H_2(g)^*$	**9.63E-01**	**1.23E+00**	**1.50E+00**	**1.78E+00**
$NaF(g)$	2.59E-11	1.65E-10	9.14E-10	4.42E-09
$Na_2F_2(g)$	6.83E-12	4.84E-11	2.93E-10	1.54E-09
$Na_3F_3(g)$	3.10E-15	3.53E-14	3.31E-13	2.60E-12
NaF^*	**1.00E+00**	**1.00E+00**	**1.00E+00**	**1.00E+00**
Na_2C_2	0.00E+00	0.00E+00	0.00E+00	0.00E+00
Na	5.64E-17	1.08E-15	1.03E-14	5.39E-14
NaH	1.53E-17	2.21E-16	1.61E-15	6.58E-15
C^*	**9.82E-01**	**1.11E+00**	**1.25E+00**	**1.39E+00**

A.3.5 - Figure 3.5: Equilibrium Products of Ethane-Pb Reaction

T (K)	773.15	798.15	823.15	848.15	873.15
C(g)	5.50E-41	2.00E-39	5.83E-38	1.39E-36	2.74E-35
C2(g)	1.95E-47	1.34E-45	7.10E-44	2.95E-42	9.84E-41
C3(g)	5.40E-45	3.47E-43	1.72E-41	6.68E-40	2.08E-38
C4(g)	3.74E-56	5.27E-54	5.46E-52	4.24E-50	2.53E-48
C5(g)	2.10E-56	3.26E-54	3.69E-52	3.11E-50	2.00E-48
C60(g)	2.96E-182	9.29E-176	1.01E-169	4.06E-164	6.36E-159
CH(g)	4.94E-35	1.03E-33	1.76E-32	2.53E-31	3.09E-30
CH2(g)	4.14E-24	3.24E-23	2.20E-22	1.32E-21	7.00E-21
CH3(g)	1.55E-11	3.92E-11	9.17E-11	2.00E-10	4.08E-10
CH4(g)	**8.67E-01**	**7.64E-01**	**6.62E-01**	**5.62E-01**	**4.70E-01**
C2H(g)	1.96E-26	2.38E-25	2.47E-24	2.20E-23	1.70E-22
C2H2(g)	1.63E-13	6.17E-13	2.12E-12	6.63E-12	1.91E-11
C2H3(g)	7.07E-18	3.19E-17	1.28E-16	4.65E-16	1.53E-15
C2H4(g)	3.24E-08	5.53E-08	8.88E-08	1.35E-07	1.93E-07
C2H5(g)	5.61E-14	1.29E-13	2.71E-13	5.28E-13	9.57E-13
C2H6(g)	9.64E-06	9.08E-06	8.25E-06	7.23E-06	6.14E-06
H(g)	1.51E-12	4.90E-12	1.47E-11	4.12E-11	1.08E-10
H2(g)	**1.27E+00**	**1.47E+00**	**1.68E+00**	**1.88E+00**	**2.06E+00**
Pb2(g)	4.15E-16	1.82E-15	7.30E-15	2.69E-14	9.19E-14
Pb(CH3)4(g)	2.60E-37	9.36E-37	2.87E-36	7.62E-36	1.78E-35
Pb(C2H5)4(g)	5.22E-54	2.03E-53	6.34E-53	1.61E-52	3.44E-52
PbH(g)	2.24E-12	7.08E-12	2.08E-11	5.67E-11	1.46E-10
Pb(H3)(Tg)	9.11E-21	3.28E-20	1.07E-19	3.20E-19	8.79E-19
C	**1.13E+00**	**1.24E+00**	**1.34E+00**	**1.44E+00**	**1.53E+00**
Pb(l)	**1.00E+00**	**1.00E+00**	**1.00E+00**	**1.00E+00**	**1.00E+00**

Appendix B: Generic Output from the HSC® Code

Two iterations of the code are included below. The run in question looks at how ethane will break down into the various compounds listed. The pressure (20 MPa) and temperatures of each iteration are listed, and this run was stepping through incrementally greater temperatures. Also included in each iteration are enthalpy and entropy of reaction. The first numerical column is taken as input and 1.0 mol of ethane was given. The second column gives the calculated number of moles of each at equilibrium.

```
GIBBS 4.5 WINDOWS FOR MULTIPHASE EQUILIBRIUM CALCULATIONS
 Copyright (C) Outokumpu Research Oy, Pori Finland 1974-2001
 T.Talonen, J.Eskelinen, T.Syvajarvi and A.Roine
*****************************************************************************
Iteration  10  Gmin# =    -56.4787732362362
 §
 Temperature         298.15   K
 Pressure           200         bar
 Volume              1.223E-04 m3 ( NPT )
 Reaction enthalpy    1.326E-08 kJ
 Reaction entropy     1.165E-08 J/K
 Iterations          10      ( Limit =  100 )
                INPUT AMOUNT    EQUIL AMOUNT          MOLE FRACT    ACTIVITY  ACTIVITY
 PHASE 1:            mol               mol                           COEFFICI
 CH2(g)            0.0000E+00  1.3710E-065            1.371E-65      1.00E+00  1.371E-65
 C2H2(g)           0.0000E+00  8.0346E-028            8.035E-28      1.00E+00  8.035E-28
 C2H4(g)           0.0000E+00  9.6718E-011            9.672E-11      1.00E+00  9.672E-11
 C2H5(g)           0.0000E+00  6.0274E-026            6.027E-26      1.00E+00  6.027E-26
 C2H6(g)           1.0000E+00  1.0000E+000             1.000E+00     1.00E+00  1.000E+00
 H(g)             0.0000E+00  1.6943E-042             1.694E-42      1.00E+00  1.694E-42
 H2(g)             0.0000E+00  9.6741E-011            9.674E-11      1.00E+00  9.674E-11
 Total :          1.0000E+00  1.0000E+000


*****************************************************************************
 Iteration  11  Gmin# =    -51.2039454164481

 §

 Temperature          353.706   K
 Pressure           200         bar
 Volume              1.451E-04 m3 ( NPT )
 Reaction enthalpy    3.113E+00 kJ
 Reaction entropy     9.557E+00 J/K
 Iterations          11       ( Limit =  100 )

                INPUT AMOUNT    EQUIL AMOUNT          MOLE FRACT    ACTIVITY  ACTIVITY
 PHASE 1:            mol               mol                          COEFFICI
 CH2(g)            0.0000E+00  1.0087E-054            1.009E-54      1.00E+00  1.009E-54
 C2H2(g)           0.0000E+00  5.5212E-023            5.521E-23      1.00E+00  5.521E-23
 C2H4(g)           0.0000E+00  7.5592E-009            7.559E-09      1.00E+00  7.559E-09
 C2H5(g)           0.0000E+00  1.3007E-021            1.301E-21      1.00E+00  1.301E-21
 C2H6(g)           1.0000E+00  1.0000E+000            1.000E+00      1.00E+00  1.000E+00
 H(g)             0.0000E+00  1.5094E-035             1.509E-35      1.00E+00  1.509E-35
 H2(g)             0.0000E+00  7.5592E-009            7.559E-09      1.00E+00  7.559E-09
 Total :          1.0000E+00  1.0000E+000
```